Numerical modelling and experimental validation of pcm-to-air heat exchangers: application of ventilated building envelopes

Mohamed Dardir, Mohamed El-Mankibi, Fariborz Haghighat

Numerical modelling and experimental validation of pcm-to-air heat exchangers: application of ventilated building envelopes

IOP Conf. Series: Materials Science and Engineering **609** (2019) 032047 doi:10.1088/1757-899X/609/3/032047

Numerical modelling and experimental validation of pcm-to-air heat exchangers: application of ventilated building envelopes

Mohamed Dardir[1,*], Mohamed El-Mankibi[2], Fariborz Haghighat[1]

[1] Department of Building, Civil and Environmental Engineering, Concordia University, Canada
[2] Department of Civil and Building Engineering, Ecole Nationale des Travaux Publics de l'Etat, France
*mo_m@encs.concordia.ca

Abstract. The earlier applications of phase change material (PCM)-to-Air heat exchangers (PAHXs) reported the insufficient cooling charging energy due to system storage abilities, the profile of inlet air temperature, and the charging duration. This paper proposes a developed PAHX system for building envelope applications utilizing both convective and long-wave radiative heat transfer components. A 2D numerical model was proposed utilizing an apparent heat capacity method to represent the PCM latent thermal storage developing both convective and radiative thermal boundaries. The radiative component was developed to study the effect of the system exposure to the night-time sky during the PCM solidification period. The convective component was comprehensively developed mainly between the storage medium (PCM) and the air channel. A real-scale prototype was constructed for the whole model experimental validation. Field experiments were designed and conducted in the warm temperate climate of Lyon, France during summer. The validation criteria were proposed based on ASHRAE guideline 14. The results of the comparison between simulated data and experimentally obtained data showed that the system temperature was within the accepted range of the proposed criteria.

1. Introduction

The working principle of thermal storage with Phase Change Materials (PCMs) is the release of a large amount of energy, latent heat of fusion, during phase change process at a relatively constant range of temperatures called Phase Change Temperature (PCT) range. In some latent heat thermal energy storage systems, air is used to charge and discharge PCM with energy. During solidification of PCM (cooling charging process), heat transfers from the liquid PCM to air; then, PCM is solidified, and subsequently air is warmed. Conversely, during cooling discharging, the air is cooled and supplied to satisfy the cooling demand during the daytime. This process involves convective heat transfer between air and PCM within heat exchangers called PCM-to-air heat exchangers (PAHXs). Applications of PAHXs have been widely discussed in the literature for cooling applications. Most of the studies revealed that maintaining outlet air temperature that achieves indoor thermal comfort was a system limitation [1,2], especially in exceptionally hot climates. Accordingly, the high inlet air temperature during solidification and the insufficient difference between inlet air temperature and PCT of the system lead to a reduced cooling charging power and low system storage capacity [3,4].

The main concept of the entire research is to increase the cooling storage ability of a developed PCM-to-air heat exchanger unit through magnifying the radiative thermal loss during PCM solidification process while the applications of building envelopes in the hot desert climate. The practical application of the proposed system is the direct free cooling by supplying the cooled air to occupied spaces. In case the cooled air could not satisfy the cooling loads, the cooled air can be introduced to the active cooling system to reduce the energy consumption required for cooling. The

radiative component was developed to study the effect of system exposure to the night-time sky during cooling charging period. The convective component will be comprehensively developed mainly between the storage medium (PCM) and the air channel. The objective of this paper is to develop the numerical model of the proposed PAHX system. This model consisted, mainly, of four components: the conduction heat transfer model between system elements, the thermal storage model (PCM model), the long-wave radiative heat transfer model, and the convective heat transfer model. The numerical model was validated against experimentally obtained data.

2. System Design

The proposed system is a PAHX system that consists of four heat transfer media (PCM, encapsulation material, air, and glazing material). As presented in Figure 1, the main concept of the system is to promote PAHX applications for building envelopes by arranging the PCM panels side by side to face the exterior. Thus, the system is exposed to the solar radiation during the daytime, and to the sky during night-time to magnify the effect of the long-wave radiative exchange between the PCM panels and black sky. The targeted heat exchange between the PCM panels and air occurs at the inner air channel (below the PCM panels). An outer air cavity is created by adding a glazing panel over the system to limit the effect of the convective heat exchange with the ambient temperature. Thus, the study of the standalone effect of the long-wave radiation can be relevant and reliable.

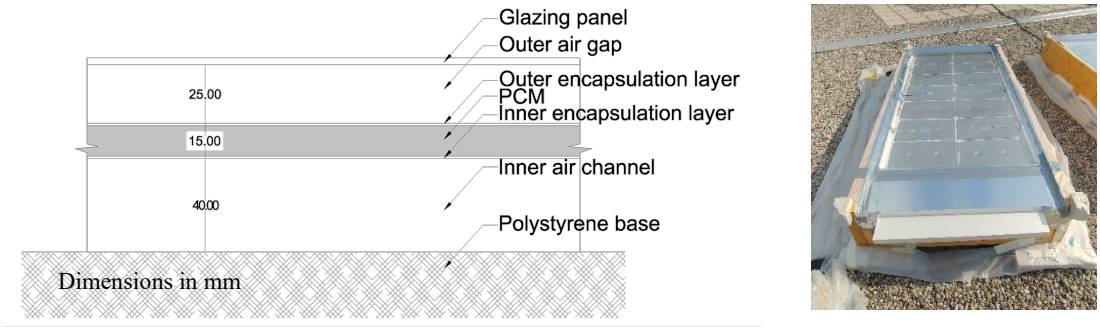

Figure 1. Developed PAHX model design for building envelope applications

3. Numerical Modeling

The main assumption of the developed numerical model is to follow the energy balance approach which depends on defining a number of control volumes of the spatial domain. The whole domain can be represented by the nodal discretization in either single or multi-dimensional analysis grid. The general energy balance equation of the system can be presented in 2D form as:

$$\rho\, c_p\, \partial T/\partial t = k\left(\partial^2 T/\partial x^2 + \partial^2 T/\partial y^2\right) \tag{1}$$

where the first order differential term $(\partial T/\partial t)$ is the temperature change in the time domain, the second order differential terms $(\partial^2 T/\partial x^2\,,\, \partial^2 T/\partial y^2)$ are the heat flux in X and Y directions, k is thermal conductivity, ρ is the density, and c_p is the material heat capacity. Generally, heat storage is represented by the increase in heat capacity values. For representing the thermal storage inside PCM, the apparent change in heat capacity values was monitored by tracking the change in temperature corresponding to the change in latent heat during phase change. Various values of heat capacity could be inferred according to Eq. 2.

$$C_p = \begin{cases} C_s & T_{pcm} < T_s \quad solid\ phase \\ L/(T_s - T_l) + (C_s + C_l)/2 & T_s < T_{pcm} < T_l \quad mushy\ region \\ C_l & T_{pcm} > T_l \quad liquid\ phase \end{cases} \tag{2}$$

Where C_s, C_l are the heat capacity in the solid and liquid phase respectively, T_s, T_l are temperature range of phase change, and L is the latent heat of fusion during phase change. This method is called

the apparent heat capacity method. The main assumption of this method is that the heat of fusion is uniformly released/absorbed during the entire phase change process [5]. In other words, it can be assumed that the heating/cooling rate is constant throughout the phase change process. The formation of the nodal discretization was proposed for all heat transfer media. The model was analyzed in 2D: X direction (direction of air flow), and Y direction (perpendicular to air flow). Resolution of analysis grid was represented by a number of nodes in both X and Y directions. The model assumed typical thermal behavior along the system height in the Z direction.

3.1. Thermal Network

The thermal-electrical analogy was used to represent the heat transfer among the system elements. The ambient thermal boundary conditions were long-wave radiation, convection, and solar radiation. The heat transfer media were airflow channel, encapsulation layers, PCM, outside air cavity and glazing layer. The thermal network of the system, presented in Figure 2, includes conductive (in case of no flow) and fluid flow boundaries inside the air channel, convective boundaries between inner encapsulation layer and air channel, conductive boundaries inside PCM, encapsulation, and glazing layers, convective boundaries between outer encapsulation and glazing layers, and air gap, and both convective and radiative boundaries between outer encapsulation and glazing layers, and the ambient environment. As claimed in literature, the natural convection inside PCM can be neglected in flat encapsulation with relatively small thicknesses, especially in horizontal configurations [6]. The long-wave radiation heat exchange between outer encapsulation and glazing layers was taken into consideration. Also, solar and long-wave radiation transmissivity of the glazing layer was considered.

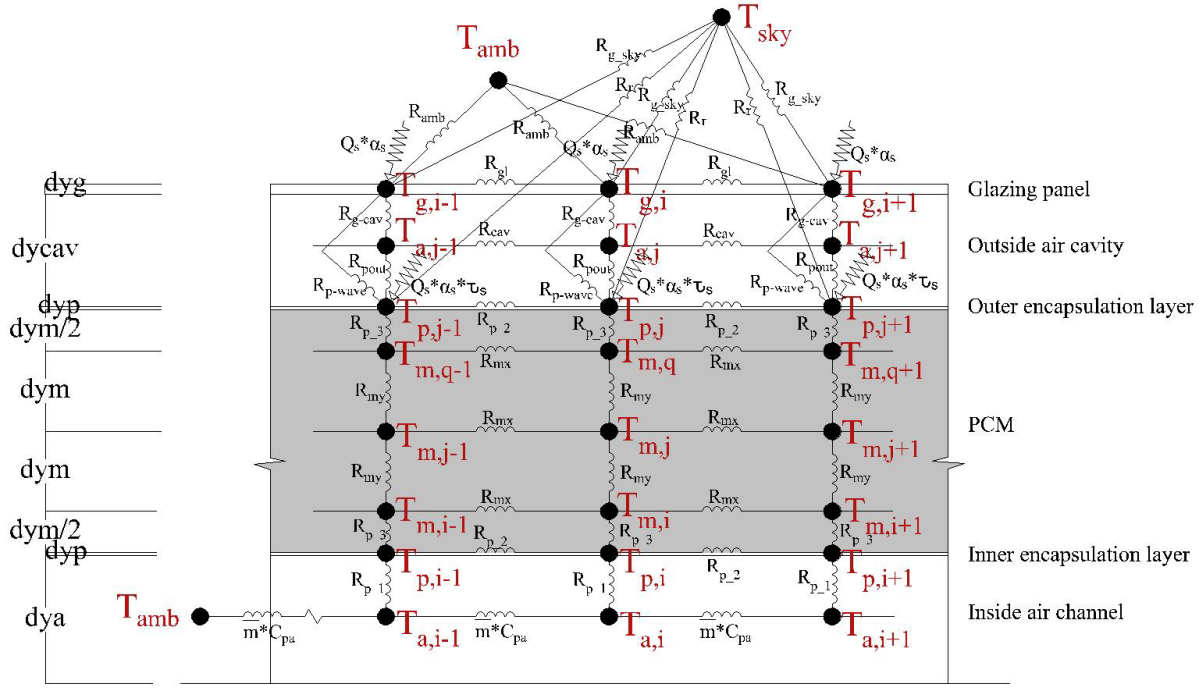

Figure 2. The thermal network of the proposed PAHX system

All energy equations of the system were formulated using the finite difference technique and expressed in an implicit form utilizing the thermal-electrical analogy. The set of heat equations was coded and numerically solved using MATLAB 2015 and SimuLink environment. All ambient conditions were used as inputs in the MATLAB program; these ambient conditions can be user-defined or real data from a weather data file.

3.2. Convection Heat Transfer Model

The convective heat transfer coefficients were calculated for the inner channel (h_{in}), the glazing layer (h_{out}), and the air cavity (h_{cav}) according to the general Eq. 3.

$$Nu_D = h \,.\, D_h / k \tag{3}$$

Where Nu : Nusselt number, D_h: the hydraulic diameter, k: air thermal conductivity. The model was configured to adapt the calculations for convective heat transfer coefficients according to air velocity values, system configuration, system orientation, and wind direction. Nusselt number was calculated each time step according to the convection mode (free, forced, or mixed convection). Various correlations for the Nusselt number were considered due to the mode of convection. For all air layers, the Nusselt number was calculated according to the possible driving forces (buoyancy and wind-driven forces). Both free and forced convection models were considered and the ratio (Gr/Re^2) was evaluated to decide which driving force was dominating; where Gr is the Grashof number representing the free convection driving forces, and Re is Reynolds number representing the forced convection driving forces. The model automatically altered among different cases of free, forced or mixed convection scenarios according to air velocity values inside the air channel.

3.3. Radiation Heat Transfer Model

The system has three radiative heat transfer components: h_r (the radiative heat transfer coefficient between outer encapsulation and the sky in case of glazing long-wave transmittance), h_g (the radiative heat transfer coefficient between the glazing and the sky), and h_w (the radiative heat transfer coefficient between the outer encapsulation and the glazing). All the radiative heat transfer coefficients were calculated according to the Stephan-Boltzmann equation. The radiative heat exchange was considered by the radiative power assuming the encapsulation layer and glazing layer as grey surfaces, and the sky as a black body. The radiative heat exchange between the encapsulation and the sky was calculated by:

$$h_r.A.\left(T_p - T_{sky}\right) = \varepsilon_p.\tau_g.\sigma.F.(T_p^4 - T_{sky}^4) \tag{4}$$

Where ε_p is the surface emissivity of the encapsulation layer, τ_g is the glazing long-wave transmittance, σ is Stephan-Boltzmann constant, F is the view factor to the sky (it is assumed to be 1), A is the hemispherical area of the node where the multi-directional radiative exchange occurs, and it is assumed to be equal to $(\pi.S)$ [7], where S is the node surface area, T_p, T_{sky} are the temperature of the encapsulation layer and the sky in kelvins respectively. Mostly, the glazing transmittance was set to zero because most of the glazing types are opaque to long-wave thermal radiation. Similarly, the radiative heat exchange between the glazing layer and the sky and the radiative heat exchange between the encapsulation layer and the glazing layer were considered.

4. Experimental Prototype

The field experiment was designed for the proposed PAHX system under real conditions to validate the numerical model. The experiment was conducted at the Building and Civil Engineering Laboratory (LGCB), Ecole Nationale des Travaux Publics de l'Etat (ENTPE) in the warm temperate climate of Lyon, France during summer 2018. The experimental prototype was constructed on the roof of the laboratory building to provide full exposure to the sky conditions. All the weather conditions, measurements, and records were monitored by ENTPE weather station. The physical prototype was made of wood frames as main structural elements and polystyrene sections to form the air channel. The prototype, shown in Figure 1, is 2,610 × 1,210 mm as external dimensions. The internal air channel was 1,060 mm in width and 40 mm in depth. Entry and exit regions were designed to regulate the supply airflow. The glazing panels were 3 mm transparent polymethyl methacrylate (PMMA) thick panels with dimensions of 2,100 × 1,000 mm. They were designed to totally cover the PCM panels and form an airtight gap with a depth of 25 mm. The used PCM panels were macro-encapsulated organic PCM RT44HC, a product of RUBITHERM [8] with a phase change temperature range of 40˚C - 44˚C, and a heat storage capacity of 250 kJ/kg. 14 PCM panels were used with dimensions of 450 × 300 × 15 mm/panel. Three parameters were monitored using temperature surface sensors and

velocity meters: PCM panels surface temperature, air temperature inside the channel, and inner channel air velocity. All sensors were connected to a compact data acquisition platform that easily transmitted the signals from the sensors to the LabVIEW software.

5. Experimental Validation

The validation investigations were conducted based on ASHRAE guideline 14 of energy measurements [9]. The guideline describes the uncertainty of the numerical model using two criteria: Normalized Mean Bias Error (NMBE), and Coefficient of Variation of Root Mean Square Error (CVRMSE). They are calculated according to Eqs. 5 and 6. For detailed calibrated simulations, this guideline claims that the numerical models are calibrated with the reference data when NMBE is within ±10%, and CVRMSE is below 30%.

$$NMBE = \Sigma_{i=1}^{n}(y_{s(i)} - y_{ref(i)})/(\bar{y}_{ref} \times n) \times 100 \quad (5)$$

$$CVRMSE = \left[\sqrt{\Sigma_{i=1}^{n}(y_{s(i)} - y_{ref(i)})^2/n}\right]/\bar{y}_{ref} \times 100 \quad (6)$$

Where y_s is the numerically simulated values, y_{ref} is the reference values where are the experimental measurements at the same time instance, $\bar{y}_{ref}$ is the average of the measured values, and n is the number of measurements per investigation. The validation of the entire model was conducted by comparing the numerical results with the experimentally obtained data. The numerical simulations were designed to meet the exact configuration, weather conditions, and procedures of the experiment. The investigation was conducted for a complete cycle of solidification and melting which provides a 24-hour application. The results, shown in Figure 3, of the model validation reveal that NMBE is -1.7%, and CVRMSE is 7.1% which is within the accepted calibration range of ASHRAE guideline 14.

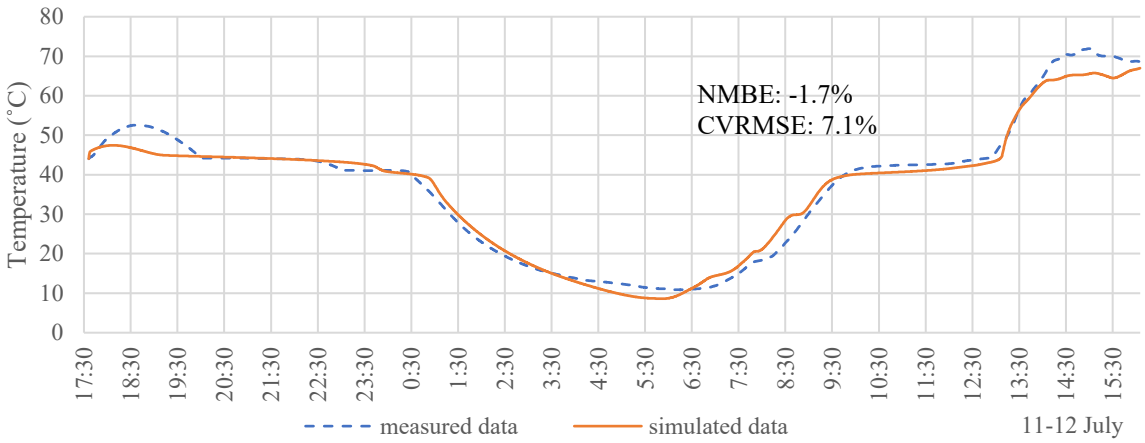

Figure 3. The temperature of PCM panel inner surface while whole model validation

6. Parametric Analysis

A numerical investigation was conducted to assess the thermal response of the model to the air velocity values inside the air channel in order to monitor the model response towards various convection modes. The above-mentioned experimental configuration was considered. The initial temperature of the system was 25˚C; inlet air temperature varied from 10˚C to 30˚C as shown in Figure 4. The air velocity values inside the air channel varied from 0 m/s to 1.2 m/s, while other model inputs and parameters were kept unchanged. Figure 4 shows that lower air velocities promote longer solidification periods and lower system temperature. It can be inferred that at the case of no airflow (V=0) the solidification occurred mainly by radiation loss to the ambient environment. This promotes the cooling potential of applying PAHX envelope system under insufficient low temperature during

cooling charging. Also, during the melting process with no airflow case, solar gains increase the system temperature minimizing the thermal loss by convection to the ambient environment. It can be noticed that with air velocity values lower than 0.5 m/s, the behavior of temperature profiles was slightly different than higher values of air velocity. This is due to the change in the calculation of convective heat transfer coefficient. At lower air velocities, the model considered that free convection was dominating. At relatively higher air velocities, the model considered the mixed convection mode where both free and forced convection driving forces had an impact on the heat transfer process.

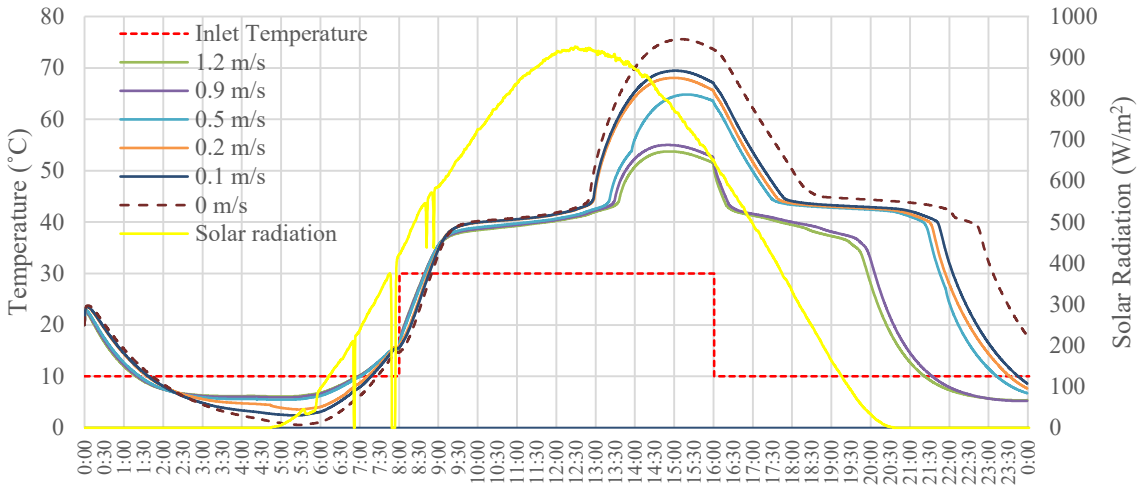

Figure 4. The influence of the air velocity (m/s) on the temperature of PCM panel

7. Conclusions

A numerical model was developed for PCM-to-air heat exchanger system for building envelope applications. Thermal storage (PCM), conduction, convection, and radiation heat transfer models were developed. A parametric analysis was conducted to assess the model response to various air velocity values. The analysis showed that lower air velocities promote longer duration with lower panel temperature during solidification and longer duration with higher panel temperature during melting. It also showed that radiation thermal loss to the ambient environment during cooling charging promoted the increased cooling charging potential of the system. Field experiments utilizing a real-scale prototype were designed and constructed in the temperate climate of Lyon, France during summer. An experimental validation for the simulated data against the experimentally obtained data was conducted using multi-criteria based on ASHRAE guideline 14. The results of the comparison showed that the numerical results of the developed model were within the accepted calibration range of the guidelines.

References

[1] Waqas A and Kumar S 2011 Energ. Buildings 43 2621-30.
[2] Arkar C and Medved S 2007 Sol. Energy 81 1078-87.
[3] Panchabikesan K, Vincent AAR and Ding YandRamalingam V 2018 Energy 144 443-55.
[4] Stritih U Butala V 2010 Int. J. Refrig. 33 1676-83.
[5] Haghighat F 2013 Applying Energy Storage in Ultra-low Energy Buildings Annex 23.
[6] Mosaffa A, Infante Ferreira C, Talati F and Rosen M 2013 Energ. Convers. Manage. 67 1-7.
[7] Incropera F DeWitt D Bergman T and Lavine A 2007 Wiley 5th ed.
[8] Rubitherm G 2019 PCM-RT Line.
[9] ASHRAE 2002 ASHRAE guideline 14 - measurement of energy and demand savings.